© 2019. Published by The Company of Biologists Ltd | Journal of Experimental Biology (2019) 222, jeb207985. doi:10.1242/jeb.207985

RESEARCH ARTICLE

C-Type allatostatin and its putative receptor from the mud crab serve an inhibitory role in ovarian development

An Liu, Fang Liu, Wenyuan Shi, Huiyang Huang*, Guizhong Wang and Haihui Ye*

ABSTRACT

C-Type allatostatins are a family of peptides that characterized by a conserved unblocked PISCF motif at the C-terminus. In insects, it is well known that C-type allatostatin has a potent inhibitory effect on juvenile hormone biosynthesis by the corpora allata. C-Type allatostatin has been widely identified from crustacean species but little is known about its roles. Therefore, this study investigated the tissue distribution patterns of C-type allatostatin and its putative receptor in the mud crab *Scylla paramamosain*, and further explored its potential effect on vitellogenesis. Firstly, cDNAs encoding C-type allatostatin (*Sp-AST-C*) precursor and its putative receptor (*Sp-AST-CR*) were isolated. Subsequently, RT-PCR revealed that *Sp-AST-C* was mainly expressed in the nervous tissue, middle gut and heart, whereas *Sp-AST-CR* had extensive expression in all tissues tested except the eyestalk ganglion and hepatopancreas. In addition, *in situ* hybridization in the cerebral ganglion showed that *Sp-AST-C* was localized in clusters 6 and 8 of the protocerebrum, clusters 9, 10 and 11 of the deutocerebrum, and clusters 14 and 15 of the tritocerebrum. Whole-mount immunofluorescence revealed a similar distribution pattern. Synthetic *Sp*-AST-C had no effect on the abundance of *S. paramamosain* vitellogenin (*Sp-Vg*) in the hepatopancreas and ovary *in vitro* but significantly reduced the expression of its receptor (*Sp-VgR*) in the ovary in a dose-dependent manner. Furthermore, *Sp-VgR* expression, vitellin content and oocyte diameter in the ovary were reduced 16 days after the first injection of *Sp*-AST-C. Finally, *in situ* hybridization showed that *Sp-AST-CR* transcript was specifically localized in the oocytes, which further indicated that the oocytes are the target cells for *Sp*-AST-C. In conclusion, our results suggested that the *Sp*-AST-C signaling system is involved in the regulation of ovarian development, possibly by directly inhibiting the uptake of yolk by oocytes and obstructing oocyte growth.

KEY WORDS: Neuropeptide, Vitellogenesis, Endocrine

INTRODUCTION

The allatostatins (ASTs) are the most abundant neuropeptides in arthropods, which were named because of their inhibitory effect on juvenile hormone (JH) synthesis by the corpora allata in insects (Stay and Tobe, 2007). Based on their distinct structural differences, ASTs are subdivided into three different families: A-type, B-type and C-type (Stay and Tobe, 2007; Verlinden et al., 2015). A-type ASTs, typified by the conserved pentapeptide C-terminal sequence Y/F-X-F-G-L/Iamide, were first discovered in the cockroach *Diploptera punctata* (Pratt et al., 1989); B-type ASTs, which have a conserved W(X_6)Wamide at the C-terminus, were first identified in the cricket *Gryllus bimaculatus* (Lorenz et al., 1995; Lorenz et al., 1999); C-type ASTs, which are characterized by a non-amidated C-terminal pentapeptide PISCF motif, a pyroglutamine blocked amino (N)-terminus and a disulfide bridge between the Cys residues located at positions 7 and 14, were first isolated in the tobacco hornworm *Manduca sexta* (Kramer et al., 1991). The precursors encoded by A-type and B-type AST genes can produce from three to 14 structurally related peptides; in contrast, the known C-type AST genes only encode a single C-type AST peptide (Stay and Tobe, 2007). To date, it is known that there exist several paralogs of the C-type AST in both insects and crustaceans, which are termed AST CC and CCC (Veenstra, 2009; Veenstra, 2016). Structurally, the C-type AST peptide is similar to the mammalian somatostatin (Veenstra, 2009). In recent years, a growing number of C-type AST peptide paralogs and structurally related peptides have been identified in other insect species and crustaceans with the application of mass spectrometry and next-generation sequencing technology (Ma et al., 2009; Dickinson et al., 2009; Stemmler et al., 2010). For instance, based on transcriptome data, two genes that encode a C-type AST peptide and a C-type AST-like peptide were identified in the mud crab *Scylla paramamosain* (Bao et al., 2015); however, the physiological roles of these peptides remain to be determined.

Previous studies have clearly demonstrated that C-type ASTs are pleiotropic peptides that are involved in many physiological activities (Verlinden et al., 2015). In the mosquito *Aedes aegypti*, C-type AST plays an inhibitory role in JH biosynthesis (Li et al., 2004) and metamorphosis (Li et al., 2006). The mechanism underlying this inhibition was recently revealed: by blocking the citrate mitochondrial carrier that transports citrate from the mitochondria to the cytosol, C-type AST could obstruct the production of cytoplasmic acetyl-CoA to further inhibit JH synthesis (Nouzova et al., 2015). It has been reported that C-type ASTs also mediate the spontaneous contractions of the foregut in the tomato moth, *Lacanobia oleracea* (Matthews et al., 2007), and stimulate the release of proteases from the gut in the red flour beetle, *Tribolium castaneum* (Audsley et al., 2013). In *Drosophila melanogaster*, C-type AST was shown to be involved in the modulation of nociception and immunity (Bachtel et al., 2018), and seasonal evening activity (Diaz et al., 2019). In addition, a regulatory role of C-type ASTs on feeding behavior was studied in the fall armyworm, *Spodoptera frugiperda* (Oeh et al., 2000). In contrast to insects, the function of C-type AST peptides in crustaceans is poorly understood. Currently, studies on their physiological roles have been reported in the American lobster, *Homarus americanus*, and the Jonah crab, *Cancer borealis*, which demonstrated that both C-type AST and C-type AST-like peptides were capable of modulating the output of the cardiac neuromuscular system and stomatogastric ganglion in *H. americanus* and *C. borealis*, respectively (Ma et al., 2009; Dickinson et al., 2009; Wiwatpanit et al., 2012).

College of Ocean and Earth Sciences, Xiamen University, Xiamen 361102, China.

*Authors for correspondence (haihuiye@xmu.edu.cn; huiyang@xmu.edu.cn)

H.Y., 0000-0002-3898-5867

Received 29 May 2019; Accepted 23 September 2019

The identification of receptors is important to better understand the functions of C-type ASTs. In *D. melanogaster*, two C-type AST receptors were first reported by Kreienkamp et al. (2002). Subsequently, receptors have been identified in other insects, including the silkworm, *Bombyx mori* (Yamanaka et al., 2008), *A. aegypti* (Mayoral et al., 2010), and *T. castaneum* (Audsley et al., 2013). In addition, two C-type AST receptors were characterized in a crustacean, *H. americanus* (Stanhope et al., 2016; Walsh et al., 2017). Interestingly, the C-type AST receptor gene in *D. melanogaster* and *H. americanus* is duplicated; it appears that the two genes might take on distinct functions as they have different expression patterns (Bachtel et al., 2018; Diaz et al., 2019; Stanhope et al., 2016; Walsh et al., 2017; for review, see Verlinden et al., 2015). As with C-type AST, the sequence of the known C-type AST receptors showed a high identity to the mammalian somatostatin receptors (Kreienkamp et al., 2002). The similarity between C-type AST peptide/receptors and somatostatin peptide/receptors suggests that C-type AST and somatostatin have a common molecular ancestor (Veenstra, 2009). This phenomenon may provide an advantage in the future identification of C-type AST receptor genes in other species.

Vitellogenesis is a crucial process in the reproduction of female crustaceans. In brachyuran crabs, vitellogenin (Vg) synthesis occurs in the hepatopancreas and ovary, although the hepatopancreas is the main synthesis site (Zmora et al., 2007; Huang et al., 2017). The oocyte takes in Vg by endocytosis, which is mediated by the Vg receptor (VgR; Warrier and Subramoniam, 2002). This process is under the control of neurotransmitters (e.g. 5-hydroxytryptamine, octopamine and dopamine), neuropeptide hormones (e.g. crustacean hyperglycemic hormone family peptides), opioid peptides (e.g. enkephalin) and steroid hormones (e.g. ecdysone and methyl famesoate) (reviewed by Nagaraju, 2011). Methyl famesoate (MF), a structurally similar hormone to insect JH, was shown to play a key role in the regulation of crustacean vitellogenesis (Miyakawa et al., 2014). To date, the C-type AST signaling system has been poorly studied in crustaceans. The objectives of this study were to describe the distribution patterns of C-type AST and its receptor in tissues of the mud crab *S. paramamosain* Estampador 1949, and to investigate whether the *Sp*-AST-C signaling system is implicated in regulating vitellogenesis. We first isolated the full-length cDNA of both *Sp-AST-C* and its receptor *Sp-AST-CR*, and subsequently identified their tissue expression profiles by reverse transcription PCR (RT-PCR), *in situ* hybridization and immunofluorescence. Based on the tissue distribution of *Sp-AST-CR* and its expression pattern in the ovary, we hypothesized that AST-C might have an inhibitory role in vitellogenesis by affecting *Sp-Vg* or *Sp-VgR* expression in the ovary. Thus, we performed both *in vitro* and *in vivo* experiments to examine the effect of synthetic *Sp*-AST-C on ovarian development.

MATERIALS AND METHODS

Animals

The collection and handling of the animals in this study was carried out in accordance with the guidelines for the care and use of laboratory animals at the Xiamen University, China.

Vitellogenesis of *S. paramamosain* can be divided into three stages (Huang et al., 2014) and crabs at each stage can be easily distinguished by the color of the ovaries: at the previtellogenic stage, the ovaries are white or milk-white; at the early vitellogenic stage, the ovaries are pale yellow to yellow in color; at the late vitellogenic stage, the ovaries are orange to reddish-orange in color. Mud crabs at the previtellogenic stage (body mass 145.6±25.3 g, carapace width 9.3±1.44 cm), early vitellogenic stage (body mass 304.7±32.3 g, carapace width 12.8±1.35 cm) and late vitellogenic stage (body mass 417.7±34.3 g, carapace width 13.6±2.23 cm) were purchased from a local fish market in Xiamen city of Fujian Province, China, and then transported to the laboratory. They were housed individually in rectangular tanks filled with seawater having a salinity of 28 ppt for a week and the seawater was renewed every day. During this period, the crabs were fed with clams (*Ruditapes philippinarum*) and the temperature was maintained at 28±1°C. Animals were placed on ice for anesthetization before tissue dissection; 11 tissues – the eyestalk ganglion, cerebral ganglion, thoracic ganglion, Y-organ, mandibular organ, heart, middle gut, ovary, hepatopancreas, muscle and hemocytes – were collected at the early vitellogenic stage for tissue distribution analysis via RT-PCR. Ovaries from crabs (n=5) at each stage were collected for *Sp-AST-CR* expression profile analysis via real-time quantitative PCR (qPCR). Samples were immediately used for RNA extraction or stored in liquid nitrogen.

RNA extraction and molecular cloning

Total RNA was extracted from the cerebral ganglia of mature females using TRIzol reagent (Invitrogen). The quantity and quality of RNA were determined using a NanoDrop spectrophotometer (Thermo Fisher Scientific). For cDNA generation, 1 µg of individual RNA was treated with DNase I (RNase-free DNase I, Invitrogen) to eliminate potential genomic DNA contamination. Subsequently, the RNA was reverse transcribed with a RevertAid First Strand cDNA Synthesis Kit (Fermentas) utilizing random primers as per the manufacturer's protocol. The cDNA generated was diluted fourfold and stored at −80°C until use.

Two cDNA fragments encoding putative *Sp-AST-C* and *Sp-AST-CR* were identified based on transcriptome data for the cerebral ganglia (Bao et al., 2015). The full-length cDNA of *Sp-AST-C* and *Sp-AST-CR* was obtained using a SMART™ RACE cDNA amplification kit (Clontech) according to the manufacturer's instructions. Primer sequences used for molecular cloning are shown in Table 1. The PCR products were separated by 1.0% agarose gel electrophoresis and detected using SYBR Green (Thermo Fisher Scientific). After gel purification, PCR products were ligated into pMD19-T vector for sequencing (Sangon Biotech) and the full-length cDNA of *Sp-AST-C* and *Sp-AST-CR* was assembled.

Predicted protein sequences were established using ORF finder, while the possible presence of signal peptides were checked using Signal P 4.0 and transmembrane domains were predicted by transmembrane prediction server TMHMM. Convertase cleavage sites and mature peptide of *Sp*-AST-C were identified based on previously described rules (Veenstra, 2016). Protein sequence alignments of *Sp*-AST-C and *Sp*-AST-CR with their homologs were established using ClustalW software.

Tissue distribution of *Sp-AST-C* and *Sp-AST-CR*

The distribution profiles of *Sp-AST-C* and *Sp-AST-CR* were analyzed by RT-PCR. Briefly, cDNAs were obtained from 11 tissues of a female *S. paramamosain*: eyestalk ganglion, cerebral ganglion, thoracic ganglion, Y-organ, mandibular organ, heart, middle gut, ovary, hepatopancreas, muscle and hemocytes. Each cDNA template was then amplified with AST-C-QF/-QR or AST-CR-QF/-QR primer pairs. Meanwhile, the housekeeping gene *β-actin* was concurrently amplified with ACT-QF/-QR primers as an internal control. Additionally, the amplification of water served as a negative control. PCR was performed with an efficient Ex-Taq® DNA polymerase (Takara) under the following conditions: 94°C for 2 min, followed by 35 cycles of 94°C for 30 s, 58°C for 30 s, 72°C for 30 s and 72°C for 10 min. Finally, PCR products were resolved on 1.0%

Journal of Experimental Biology (2019) 222, jeb207985. doi:10.1242/jeb.207985

Table 1. Summary of primers used in this study

Primer	Primer sequence (5′–3′)	Target size (bp)	Application
AST-C-3F1	CACCTATCAGGACCTGCCATCTTT	806	3′RACE
AST-C-3F2	GCAAGAAGAAGAGGATGTTTG	705	3′RACE
AST-C-5R1	GCTTCGAGCTCCTCCTGGCTGGTGT	322	5′RACE
AST-C-5R2	TGGCGGGCAGGGCGTGACTCAGGGT	213	5′RACE
AST-C-QF	TCACTCGCTGCTTGTTATCCT	199	RT-PCR
AST-C-QR	AACCCCATCTCCTGCTTCA		RT-PCR
AST-C-IF	GACCCTGAGTCACGCCCTGCCCGC	239	ISH
AST-C-IR	TCCCCATCGACCTCCGCCTTCAGT		ISH
AST-CR-5R1	CACGTAGATGACGAGAGTGTTGC	1234	5′RACE
AST-CR-5R2	ACGTCCGCGATGTCCGTGTTATTG	1104	5′RACE
AST-CR-QF	CAAGGCAAAGTCCAAGGAGAAG	192	RT-PCR
AST-CR-QR	TAGGAGAGGCAGGAGGAAATCA		RT-PCR
AST-CR-IF	GTGTTGGCTGCCCTACTGG	420	ISH
AST-CR-IR	TTCCTGACGGAGTGGCTGTCCC		ISH
Vg-QF	CGCAACCGCCACTGAAGAT	204	qPCR
Vg-QR	CCACCATGCTGCTCACGACT		qPCR
VgR-QF	TTCTATACCAGGCCACTACC	185	qPCR
VgR-QR	TTTTCACTCCAAGCACACTC		qPCR
ACT-QF	CACACTTCACAGACCTTC	187	qPCR
ACT-QR	CACAATGCCATCCTCTAC		qPCR
T7	TAATACGACTCACTATAGGG		ISH
SP6	ATTTAGGTGACACTATAG		ISH

ISH, *in situ* hybridization; RT-PCR, reverse transcription PCR; qPCR, real-time quantitative PCR.

agarose gel, stained with ethidium bromide and visualized under a UV detector (Geldoc, Thermo Fisher Scientific).

In situ hybridization

RNA probes were generated by two pairs of gene-specific primers, AST-C-IF/IR and AST-CR-IF/IR, and the universal primers T7/SP6 (Table 1). The *in situ* hybridization was performed as described in our previous study (Liu et al., 2018). Briefly, samples of the cerebral ganglion and ovary were dissected from a female *S. paramamosain* at the early vitellogenesis stage, and immediately rinsed 3 times in 0.1 mol l^{-1} phosphate-buffered saline (PBS, pH 7.4). Tissues were then fixed overnight in a solution of 4% paraformaldehyde prepared in 0.1 mol l^{-1} PBS at 4°C. After rinsing 3 times with 0.1 mol l^{-1} PBS, samples were dehydrated with 75% ethanol, 85% ethanol, 95% ethanol and 100% ethanol in order, followed by treatment with xylene, then embedded in paraffin. Finally, the embedded tissues were sectioned with thickness of 7 µm for hybridization. Hybridization was carried out using DIG RNA Labeling Kit (Roche, Switzerland) and the signal was detected by alkaline phosphatase using a BCIP/NBT Chromogen kit (Solarbio, China).

Peptide synthesis

Based on the deduced amino acid sequence of the C-type AST preprohormone, the mature *Sp*-AST-C peptide (QIRYHQCYFNPISCF-OH, with a disulfide bridge present between C7 and C14) was synthesized (GL Biochem Ltd, Shanghai, China), with a purity of 98%, for the subsequent experiments.

Whole-mount immunohistochemistry

Antibody production

To map the distribution of *Sp*-AST-C peptides, a custom-produced polyclonal rabbit antibody was generated (GL Biochem Ltd). This antibody was raised against the predicted mature *Sp*-AST-C peptide conjugated via the N-terminal cysteine to keyhole limpet hemocyanin. Two months after immunizations, serum containing antibody was obtained and the antibody was purified by affinity chromatography. Finally, the specificity and efficiency of the antibody were determined and it was stored at −80°C until use.

Whole-mount immunofluorescence

Whole-mount immunofluorescence staining was performed following a method described by Christie et al. (2006). In detail, samples of the cerebral ganglion were fixed in a solution of 4% paraformaldehyde in 0.1 mol l^{-1} PBS at 4°C overnight. At the end of this period, tissues were rinsed 5 times at ∼1 h intervals at room temperature in PBS containing 0.3% Triton-X 100 (PBS-T) and then incubated for ∼72 h at 4°C in primary antibody (rabbit anti-AST-C) diluted to a final working concentration of 1:5000) Subsequently, tissues were rinsed 5 times at ∼1 h intervals at room temperature in PBS-T, followed by incubation in goat anti-rabbit IgG conjugated to Alexa Fluor® 594 (ab150080, Abcam; 1:500 dilution) for ∼24 h at 4°C. Both the primary and secondary antibody were diluted in PBS-T containing 10% normal donkey serum. Before visualization, samples were incubated in 4′,6-diamidino-2-phenylindole (DAPI, Invitrogen) buffer to label the cell nuclei. To render the samples transparent so that the fluorescence signals from the labeled cells could be easily detected, tissues were treated with scale reagent for ∼3 days (Hama et al., 2011). Finally, the samples were imaged using a Zeiss LSM780 system equipped with a 10× dipping objective lens.

In vitro effect of *Sp*-AST-C peptide on *Sp-Vg* and *Sp-VgR* expression

To test a potential effect of *Sp*-AST-C peptides on vitellogenesis of *S. paramamosain*, an *in vitro* experiment was conducted. This experiment was repeated 3 times. Briefly, female crabs at the early vitellogenic stage were anesthetized on ice for 10 min, followed by sterilization in 75% ethanol for 10 min. After that, tissues of the ovary and hepatopancreas were dissected and washed with crab saline containing penicillin G (300 IU ml^{-1}) and streptomycin (300 mg ml^{-1}) 9 times. Subsequently, the samples were cut into fragments of approximately 50 mg and placed in a well of 24-well

Journal of Experimental Biology (2019) 222, jeb207985. doi:10.1242/jeb.207985

culture plate with 500 µl L15 medium containing penicillin G and streptomycin as above for preincubation at 25°C. The experiment included four treatments: three different concentrations (10^{-5}, 10^{-6} and 10^{-7} mol l^{-1}) of *Sp*-AST-C peptide (treatments 1–3) and a control without any peptide (treatment 4); each treatment had four replicates (n=4). After a 1 h pre-incubation, the culture medium was replaced with L15 medium containing different concentrations of peptide and incubated for another 24 h. Finally, the ovarian and hepatopancreatic explants were collected for total RNA extraction and cDNA synthesis, and the expression of *Sp-Vg* (GenBank accession number: FJ812090.1) and *Sp-VgR* (GenBank accession number: KF860893.1) was detected by qPCR.

In vivo effect of *Sp*-AST-C on ovarian development

Based on the results of the *in vitro* experiment, we speculated that *Sp*-AST-C had an inhibitory role in vitellogenesis. To confirm this hypothesis, a long-term *in vivo* experiment was performed. Mud crabs at the early vitellogenic stage were randomly divided into three groups, each containing four individuals (n=4). Before injection, a group of animals was sampled as a pre-injection control. Crabs were then injected with *Sp*-AST-C peptide (10 ng g^{-1} body mass) in 100 µl crab saline once every 5 days, while the saline control received 100 µl crab saline instead. On day 16, approximately 24 h after the third injection, crabs were placed on ice for anesthetization before being killed, and samples of ovary were dissected for gene expression analysis, vitellin (Vn) measurement and histological analysis (Hemotoxylin and Eosin staining).

The content of Vn in ovary was detected by western blot with anti-Vn antibody against the swimming crab *Portunus trituberculatus* Vn (Zhang et al., 2011). Briefly, 50 mg of ovary was homogenized in 0.5 ml of extraction buffer (0.1 mol l^{-1} Tris-HCl, 0.1 mol l^{-1} NaCl, 2.5 mmol l^{-1} EDTA, 0.5% Triton X-100), followed by centrifugation

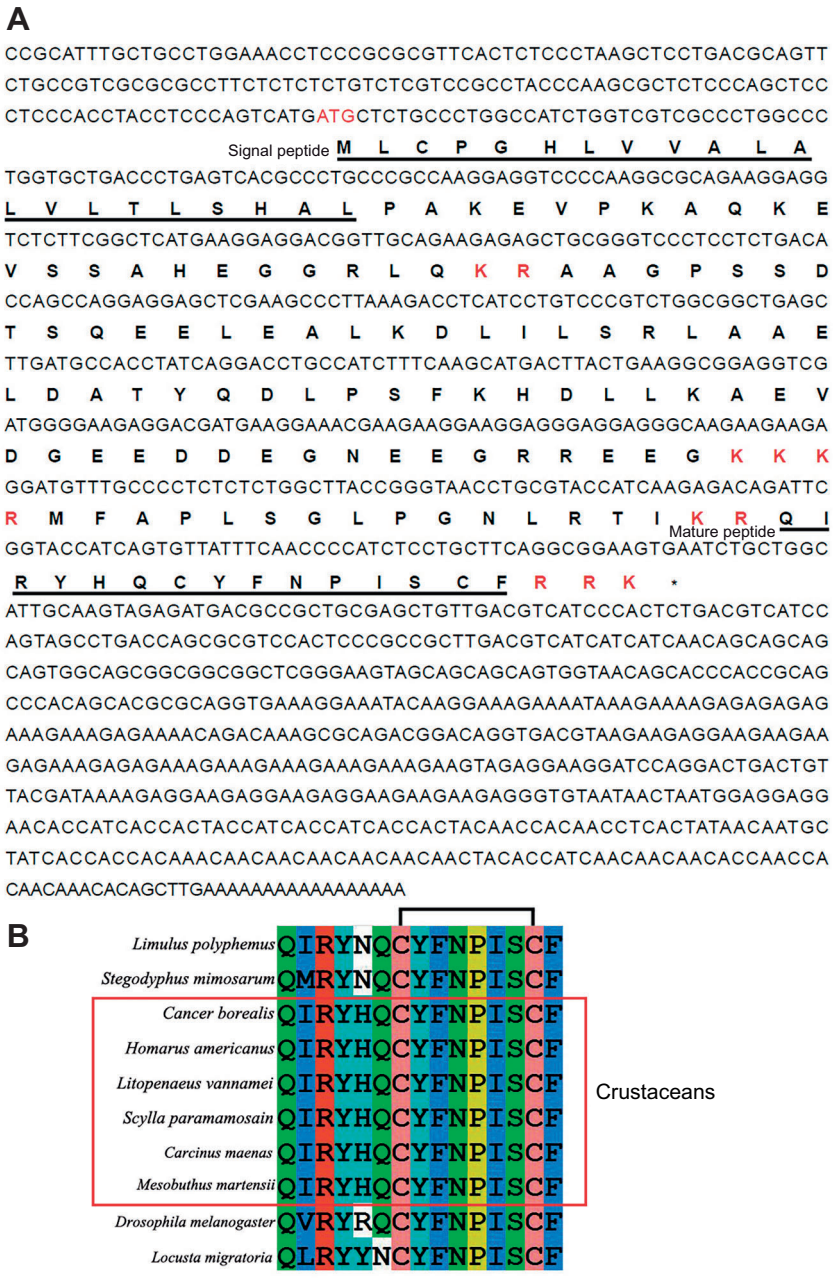

Fig. 1. *Scylla paramamosain* C-type allatostatin (*Sp-AST-C*). (A) Nucleotide and deduced amino acid sequence of *Sp-AST-C*. The ORF is shown in a single letter code below the nucleotide sequence. The signal and mature peptides are underlined; the initiation codon and the dibasic cleavage sites are indicated in red. (B) Sequence alignment of the known C-type allatostatin (AST) peptides in insects and crustaceans.

Journal of Experimental Biology (2019) 222, jeb207985. doi:10.1242/jeb.207985

at 10,000 ***g*** for 10 min at 4°C. The supernatant was subsequently collected and the amount of total protein was measured by the Bradford method. A 30 µg sample of total protein was subjected to 8% SDS-PAGE and then transferred to a PVDF membrane. The membrane was blocked in blocking buffer (PBS containing 5% BSA) for 1 h, followed by incubation with rabbit anti-Vn antibody diluted 1:1000 in blocking buffer at 37°C for 1 h, and subsequently washed 3 times in 0.1 mol l^{-1} PBS containing 0.1% Tween 20 (PBST). The membrane was then incubated in goat anti-rabbit IgG conjugated to HRP (diluted 1:1000 in PBST) for 1 h at room temperature and washed 3 times in PBST. Finally, protein bands were detected using an Easysee Western Blot kit (Transgen Biotech).

Statistical analyses

The qPCR data were calculated using the $2^{-\Delta\Delta Ct}$ method and normalized to β-actin gene expression. Subsequently, Levene's test was used for homoscedasticity and statistical significance of the data (P<0.05) was determined using one-way analysis of variance with *post hoc* Duncan's multiple comparison test (SPSS 20.0). The results are presented as means±s.e.m.

RESULTS

Sp-AST-C and *Sp-AST-CR* cDNA

By PCR and RACE methods, the full cDNA sequence of *Sp-AST-C* was cloned from cerebral ganglion cDNA of *S. paramamosain*. The complete cDNA of *Sp-AST-C* had a length of 1773 bp (GenBank accession number: MK314113). It consisted of an ORF of 450 bp that coded for a 149 amino acid precursor, flanked by 5′ and 3′ UTRs of 140 bp and 583 bp, respectively. The precursor contained a 21 amino acid signal peptide, three precursor related peptides and a mature C-type AST peptide flanked by two dibasic cleavage sites (Fig. 1A). The mature peptide (QIRYHQCYFNPISCF-OH) was 15

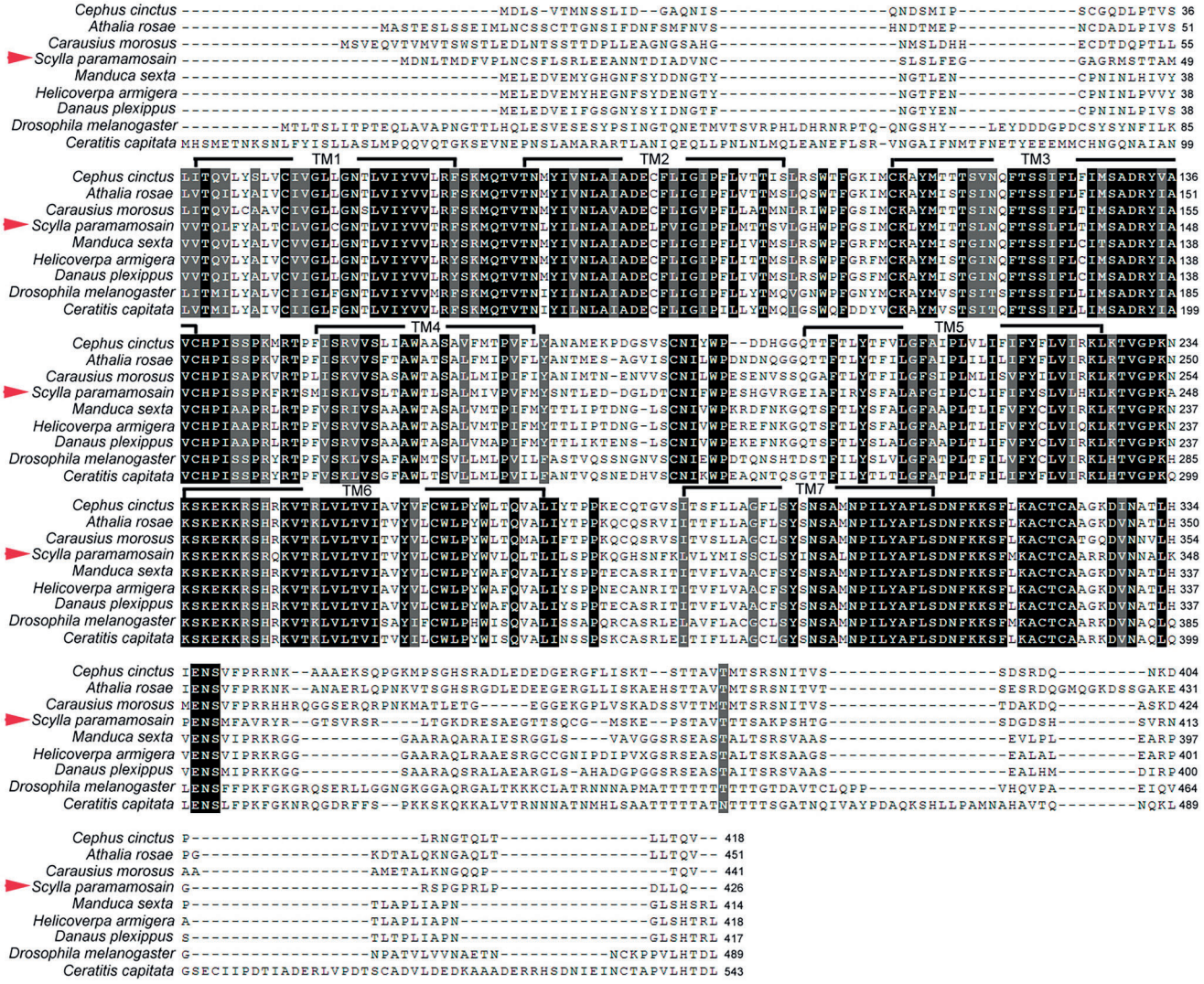

Fig. 2. Amino acid sequence of *S. paramamosain* C-type AST receptor (*Sp*-AST-CR) and its homologs. Sequence alignments of the predicted C-type AST receptor in *S. paramamosain* and of its homologs in *Cephus cinctus* (GenBank: XP_015598452.1), *Athalia rosae* (GenBank: XP_012260695.1), *Carausius morosus* (GenBank: AOV81581.1), *Manduca sexta* (GenBank: ADX66345.1), *Helicoverpa armigera* (GenBank: XP_021194801.1), *Danaus plexippus* (GenBank: OWR41004.1), *Drosophila melanogaster* (GenBank: AAL02125.1) and *Ceratitis capitata* (GenBank: XP_023159475.1). The amino acid number is indicated on the right. Conserved residues are highlighted with a black background and conservative changes have a gray background.

amino acids in length, was non-amidated and possessed two cysteine residues at positions 7 and 14 connected by a disulfide bridge (Fig. 1B).

Additionally, we isolated a fragment encoding a putative C-type AST receptor using transcriptome data for the cerebral ganglion. By 5′ RACE, the complete coding region of *Sp-AST-CR* was subsequently obtained (GenBank accession number: MK314114), containing 3309 bp with an ORF of 1281 bp that coded for a 426 amino acid protein, flanked by a 5′ UTR of 1015 bp and an incomplete 3′ UTR of 325 bp, respectively. The TMHMM transmembrane prediction server predicted that *Sp*-AST-CR contained seven transmembrane domains, like other G protein-coupled receptors (Fig. 2). Sequence alignment revealed that *Sp*-AST-CR had a high identity to the C-type AST receptor reported in *D. melanogaster* and *M. sexta*, and to other predicted insect receptors.

Expression of *Sp-AST-C* and *Sp-AST-CR* in *S. paramamosain*

To survey the tissue expression profiles of *Sp-AST-C* and *Sp-AST-CR* in *S. paramamosain*, an RT-PCR assay was performed. Our results showed that of 11 tissues detected, *Sp-AST-C* was highly expressed in the cerebral ganglion, thoracic ganglion and the middle gut, with much lower levels in the eyestalk ganglion and heart. *Sp-AST-CR* was found to be extensively expressed in the tissues of *S. paramamosain*, including the cerebral ganglion, thoracic ganglion, Y-organ, mandibular organ, heart, middle gut, ovary, muscle and hemocytes, whereas no transcript was detected in the eyestalk ganglion and hepatopancreas (Fig. 3A). In addition, the expression profile of *Sp-AST-CR* in the ovary at three vitellogenic stages, determined by qPCR (Fig. 3B), showed that it had high expression at the previtellogenic stage and that expression significantly decreased in the early and late vitellogenic stages ($P<0.01$).

Localization of *Sp*-AST-C in the cerebral ganglion of *S. paramamosain*

According to previous studies, the cerebral ganglion can be divided into the protocerebrum, deutocerebrum and tritocerebrum (see Sandeman et al., 1992). The results of *in situ* hybridization revealed that *Sp-AST-C* transcripts were localized in the cells of clusters 6 and 8 of the protocerebrum; clusters 9, 10 and 11 of the deutocerebrum; and clusters 14 and 15 of the tritocerebrum (Fig. 4A,C–E). No positive signal was detected when a sense probe was used (Fig. 4B).

C-Type AST immunoreactivity was found to be distributed throughout the cerebral ganglion (Fig. 5). There were many immunoreactive cells in clusters 6 and 8 of the protocerebrum. In the deutocerebrum, strong immunoreactivity was observed in clusters 9 and 11, while no immunoreactivity was detected in cluster 10. In addition, strong immunoreactivity was also detected in the olfactory lobe. A few immunoreactive cells were detected in clusters 14 and 15 of the tritocerebrum.

In vitro effect of synthetic *Sp*-AST-C peptide on vitellogenesis

The synthetic *Sp*-AST-C peptide was applied to the culture medium containing the explants of ovaries or hepatopancreas at the early vitellogenic stage. The qPCR results showed that *Sp*-AST-C significantly reduced the level of *Sp-VgR* transcript in the ovary in a dose-dependent manner (Fig. 6C). In contrast, the levels of *Sp-Vg* transcript in both the hepatopancreas and ovary showed no statistical difference after addition of *Sp*-AST-C peptide (Fig. 6A,B).

In vivo effect of *Sp*-AST-C peptide on Vg uptake and oocyte growth

In vivo injection of *Sp*-AST-C peptide reduced the expression of *Sp-VgR* and the content of Vn in ovary but did not affect *Sp-Vg* expression (Fig. 7). This result was confirmed by the findings of the histological analysis, which showed that the administration of *Sp*-AST-C decreased the diameter of the oocytes and the number of yolk granules (Fig. 8). In summary, the *in vivo* experiment indicated that *Sp*-AST-C could inhibit oocyte uptake of Vg and obstruct oocyte growth in *S. paramamosain* ovary.

Localization of *Sp-AST-CR* in the ovary of *S. paramamosain*

Based on histological characterization, the ovary was at the early vitellogenic stage, in which oocytes were surrounded by follicular cells, and only a few previtellogenic oocytes were observed (Fig. 9C). The antisense *Sp-AST-CR* probe gave a clear signal in the oocytes but not in the follicular cells (Fig. 9A). Interestingly, previtellogenic oocytes showed a much stronger signal than early vitellogenic oocytes. No signal was detected when a sense probe or PBS was used as a negative control (Fig. 9B). The results showed that *Sp-AST-CR* was exclusively expressed in oocytes in the mud crab ovary.

DISCUSSION

In insect species, the C-type ASTs are a group of structurally conserved peptides named because of their inhibitory effect on JH biosynthesis in the corpora allata (Kramer et al., 1991; Li et al., 2004; Li et al., 2006; Abdel-Latief and Hoffmann, 2010; Wang

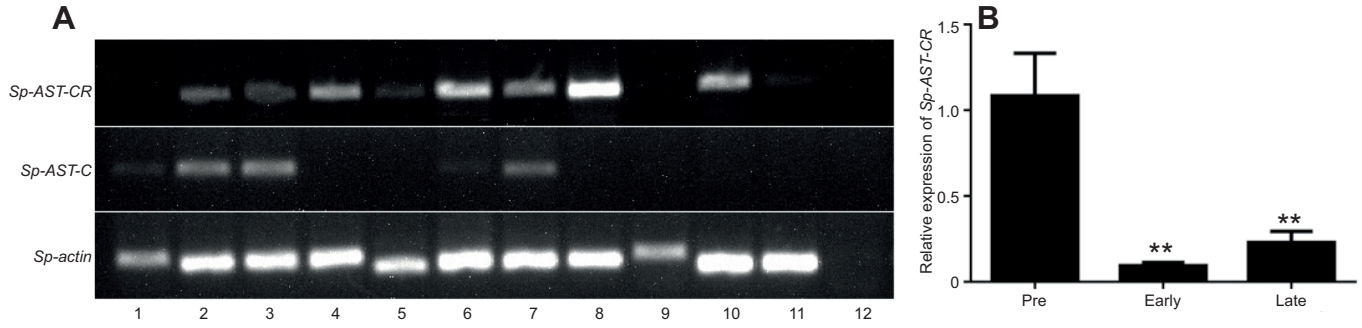

Fig. 3. Expression of *Sp-AST-C* and *Sp-AST-CR* in *S. paramamosain*. (A) The distribution of *Sp-AST-C* and *Sp-AST-CR* expression, as detected by qPCR. *Scylla paramamosain* β-*actin* was included as a control. 1: eyestalk ganglion; 2: cerebral ganglion; 3: thoracic ganglion; 4: Y-organ; 5: mandibular organ; 6: heart; 7: middle gut; 8: ovary; 9: hepatopancreas; 10: muscle; 11: hemocytes; 12: negative control (water). (B) The expression pattern of *Sp-AST-CR* in the ovary during development (previtellogenic, early vitellogenic and late vitellogenic stage). Asterisks indicate significant differences from the previtellogenic stage (**$P<0.01$).

Journal of Experimental Biology (2019) 222, jeb207985. doi:10.1242/jeb.207985

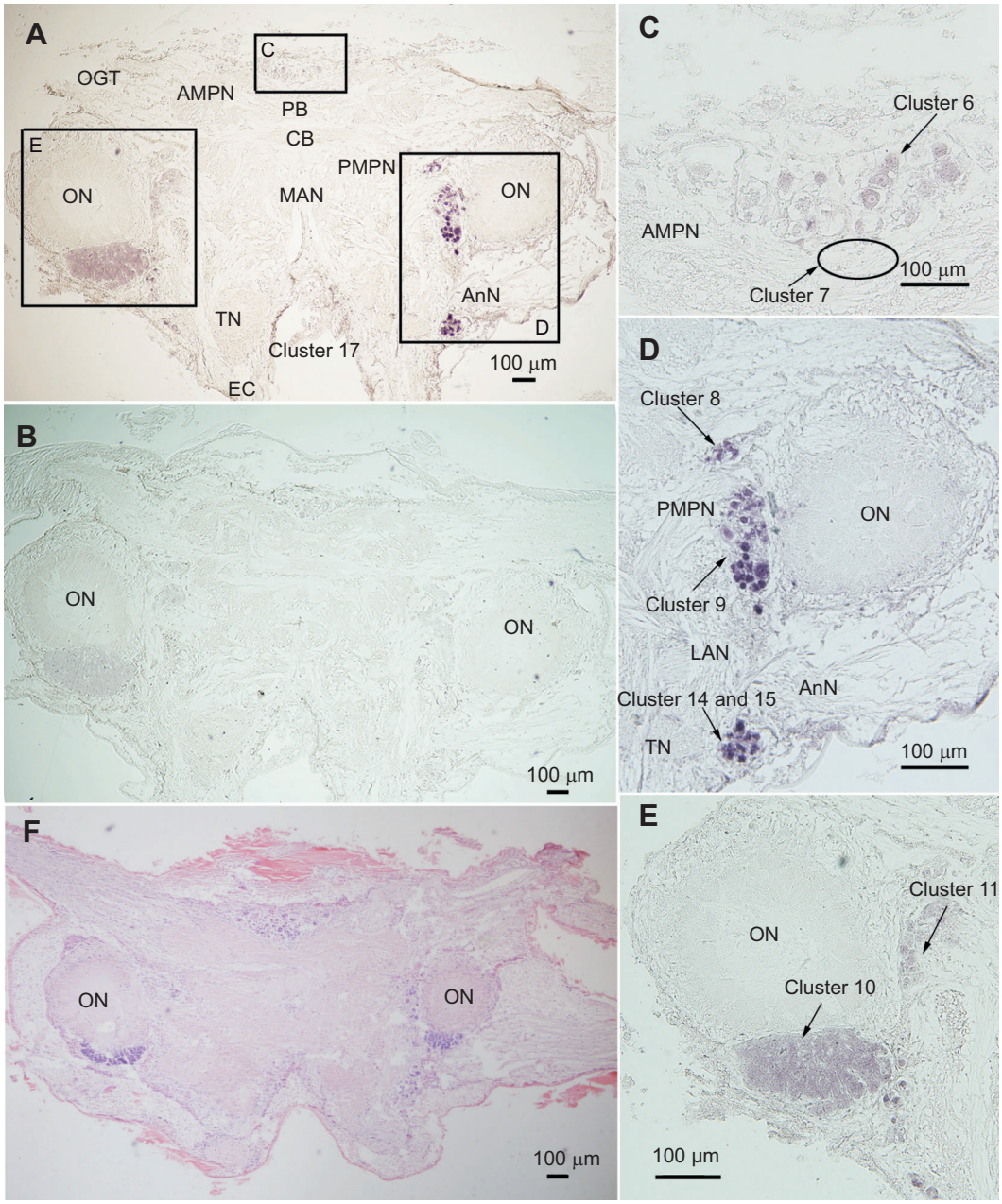

Fig. 4. Localization of *Sp-AST-C* in the cerebral ganglion of *S. paramamosain* at the early vitellogenesis stage. (A) Localization of *Sp-AST-C*-expressing cells in the cerebral ganglion using an antisense probe. (B) Negative control using the sense probe. (C–E) Enlargement of the boxed regions in A, showing *Sp-AST-C* localization in clusters 6 and 8 of the protocerebrum; clusters 9, 10 and 11 of the deutocerebrum; and clusters 14 and 15 of the tritocerebrum. (F) Hematoxylin and Eosin staining. OGT, olfactory globular tract; AMPN, anterior medial protocerebral neuropil; PMPN, posterior medial protocerebral neuropil; PB, protocerebral bridge; CB, central body; ON, olfactory lobe; MAN, median antenna I neuropil; LAN, lateral antenna I neuropil; TN, tegumentary neuropil; AnN, antenna II neuropil; EC, esophageal connectives.

et al., 2012). To date, the regulatory role of C-type ASTs on JH biosynthesis in the corpora allata has been well studied in insects (for review, see Stay and Tobe, 2007). The recent discovery in *A. aegypti* of the mode of action of C-type AST in the regulation of JH biosynthesis is a great breakthrough (Nouzova et al., 2015). It is now known that the C-type AST is also widely present in crustacean species, such *H. americanus* (Dickinson et al., 2009), the white shrimp *Litopenaeus vannamei* (Stemmler et al., 2010) and *S. paramamosain* (Bao et al., 2015); however, information on the potential functions of C-type ASTs in crustaceans is rather limited. In the present study, we describe the distribution profiles of a C-type AST and its putative receptor in the mud crab *S. paramamosain* and verified its inhibitory role in vitellogenesis.

In our previous study, we identified a fragment sequence that encoded a C-type AST precursor (*Sp-AST-C*) from our transcriptome database of *S. paramamosain* (Bao et al., 2015). By RACE PCR-based isolation, the full-length cDNA of *Sp-AST-C* was cloned from the cerebral ganglion of *S. paramamosain*. The *Sp*-AST-C precursor shared a similar basal framework with the C-type ASTs previously reported in insects and other crustaceans, which consisted of a signal peptide, three precursor-related peptides and a mature peptide (Fig. 1A). The mature peptide was 15 amino acids

Journal of Experimental Biology (2019) 222, jeb207985. doi:10.1242/jeb.207985

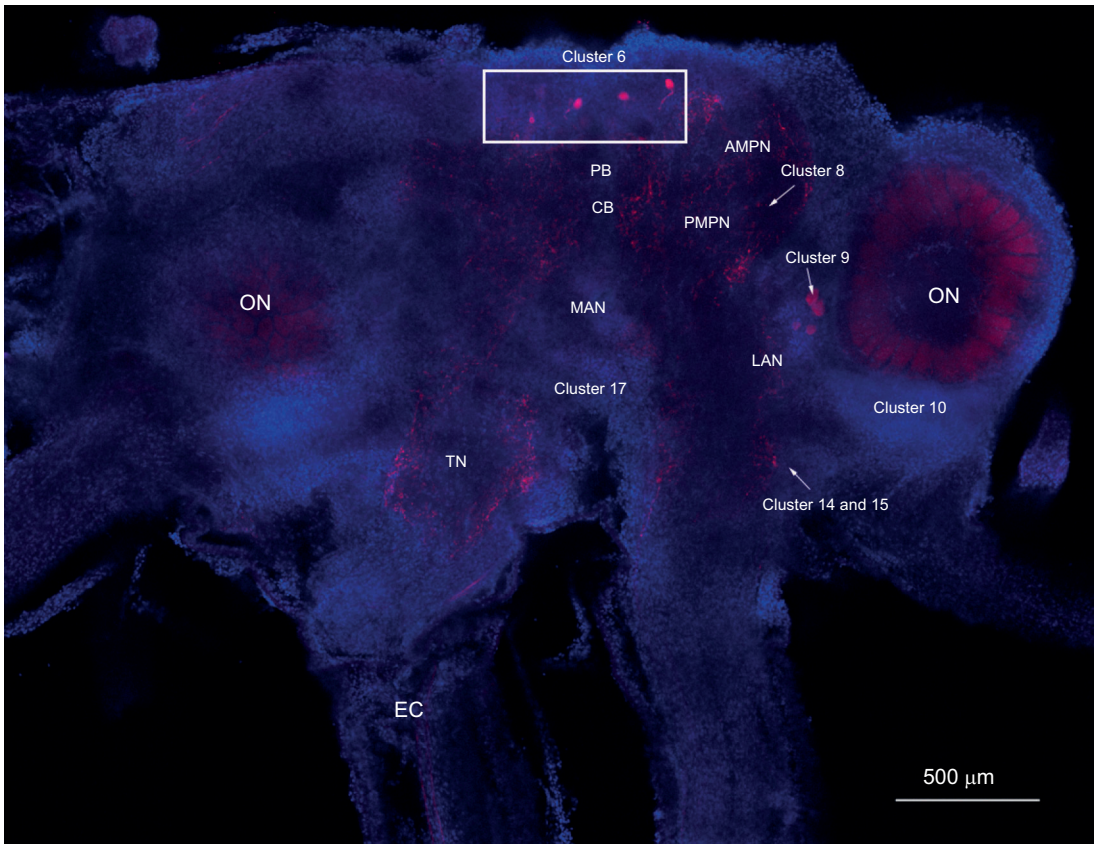

Fig. 5. Localization of C-type AST immunoreactivity (red) in the cerebral ganglion of *S. paramamosain* at the early vitellogenesis stage. Blue indicates cell nuclei labelled by DAPI. AMPN, anterior medial protocerebral neuropil; PMPN, posterior medial protocerebral neuropil; PB, protocerebral bridge; CB, central body; ON, olfactory lobe; MAN, median antenna I neuropil; LAN, lateral antenna I neuropil; TN, tegumentary neuropil; EC, esophageal connectives.

(QIRYHQCYFNPISCF-OH) in length, characterized by a PISCF-OH motif in the C-terminus (Fig. 1B). In addition, two cysteine residues at positions 7 and 14 were found in the mature peptide that were connected by an intramolecular disulfide bridge, which is an invariable feature for C-type AST family peptides (Veenstra, 2009). It has been shown that such a feature is essential for the function of C-type AST peptides (Kreienkamp et al., 2002). Three members of the C-type AST family have been identified: C, CC and CCC (Veenstra, 2009, 2016). The notable characteristics of AST-C that differ from those of the other two peptides are that it has a Pro residue in the disulfide bridge and a predicted pyroglutamate residue in the N-terminus of the mature peptide (Veenstra, 2016). Based on sequence characteristics, *Sp*-AST-C is a C-type AST peptide. Finally, sequence alignment showed that the mature peptide of C-type AST in crustaceans was identical and had high identity to the insect C-type ASTs (Fig. 1B), indicating that C-type AST is conserved among insects and crustaceans.

It was shown that the insect C-type AST receptor is related to the mammalian somatostatin/opioid receptor family (Kreienkamp et al., 2002; Olias et al., 2004). This is clear from the structural similarity of C-type ASTs to the mammalian somatostatin (Veenstra, 2009). To date, the C-type AST receptor has been studied in several insect species, e.g. *A. aegypti* (Mayoral et al., 2010), *D. melanogaster* (Kreienkamp et al., 2002) and *T. castaneum* (Audsley et al., 2013),

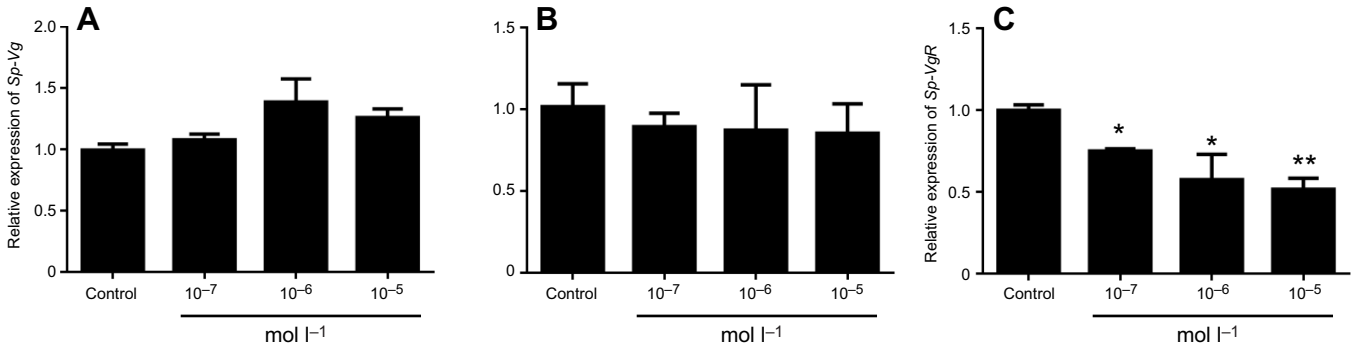

Fig. 6. Effect of synthetic *Sp*-AST-C peptide on the *in vitro* expression of *Sp-Vg* and *Sp-VgR*. (A,B) Relative expression of *Sp-Vg* in the hepatopancreas (A) and ovary (B). (C) Relative expression of *Sp-VgR* in the ovary. The samples were collected from the no-peptide control and after incubation with 10^{-7}, 10^{-6} or 10^{-5} mol l^{-1} synthetic *Sp*-AST-C peptide. Data are shown as means±s.e.m. (n=4). Asterisks indicate significant differences from control (*P<0.05; **P<0.01).

Journal of Experimental Biology (2019) 222, jeb207985. doi:10.1242/jeb.207985

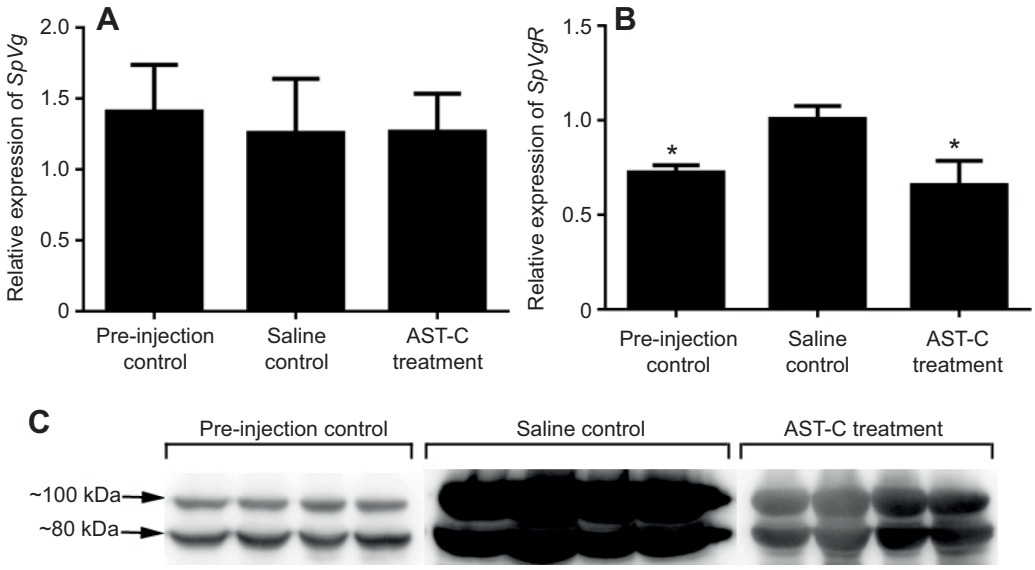

Fig. 7. *In vivo* effect of synthetic *Sp*-AST-C peptide on vitellogenesis of *S. paramamosain*. (A,B) Relative expression of *Sp-Vg* (A) and *Sp-VgR* (B) in the ovary 16 days after the first injection of synthetic AST-C peptide (see Materials and Methods). (C) Western blot showing the change in Vn content of the ovary 16 days after the first injection of synthetic *Sp*-AST-C peptide. Data are means±s.e.m. (*n*=4). Asterisks indicate significant differences from the saline control (**P*<0.05).

and one crustacean species, *H. americanus* (Stanhope et al., 2016; Walsh et al., 2017). In Diptera, there are two AST-C receptor genes that may be involved in different physiology functions. For instance, in *D. melanogaster*, it has been reported that *allatostatin-C receptor 2* is specifically involved in the regulation of immunity and nociception (Bachtel et al., 2018), and the modulation of seasonal evening activity (Diaz et al., 2019). Similarly, two putative receptors were identified in *H. americanus* (Stanhope et al., 2016). However, in *S. paramamosain*, only one putative receptor, *Sp-AST-CR*, was found by analysis of the transcriptome sequence. Like insect C-type AST receptor, this putative receptor is related to the mammalian somatostatin receptors. Furthermore, sequence alignment revealed that *Sp-AST-CR* and the insect C-type AST receptors are highly similar in the transmembrane domains (Fig. 2), which indicates that *Sp-AST-CR* encodes a C-type AST receptor in *S. paramamosain*. Nevertheless, a functional assay is needed to confirm whether this putative receptor can be activated by *Sp*-AST-C peptide.

In the insect species, C-type AST is considered to be a brain–gut peptide as it is mainly secreted by the brain and gut (Williamson et al., 2001). For instance, in *T. castaneum*, it was reported that *Tc-AST-C* is expressed in the greatest amounts in the head, with lower transcript levels in the gut, fat body and testis (Audsley et al., 2013). In the present study, RT-qPCR results showed that *Sp-AST-C* transcripts were mainly expressed in the cerebral ganglion, thoracic ganglia and gut, with much lower levels in the eyestalk ganglion and heart (Fig. 3). Such a result is largely in accordance with the findings in insect species. Similarly, the expression of C-type AST in the cerebral ganglion, eyestalk ganglion, heart and gut was recorded in *H. americanus* and *C. borealis* (Stemmler et al., 2010). The appearance of C-type AST in the nervous system revealed that *Sp*-AST-C might serve as a neuromodulator and neurohormone (Stemmler et al., 2010; Wilson and Christie, 2010). This is further supported by the localization of *Sp*-AST-C in the cerebral ganglion through *in situ* hybridization and immunofluorescence staining in the present study. Both *Sp-AST-C* mRNA and *Sp*-AST-C peptide exhibited a wide distribution in the cerebral ganglion. Interestingly, *Sp-AST-C* was expressed in cluster 10 of the deutocerebrum, where *Sp*-AST-C peptide immunoreactivity was not detected. This phenomenon might be caused by the low expression of *Sp-AST-C* in cluster 10 and the peptide being immediately secreted out as soon as it is synthesized. The extensive distribution of *Sp-AST-C* in the cerebral ganglion implies it has multiple functions, as suggested in the case of oxytocin/vasopressin-like mRNA in the blue swimming crab, *Portunus pelagicus* (Saetan et al., 2018). Based on the function of the cerebral ganglion structure, the presence of *Sp*-AST-C in clusters 6 and 8 indicated that it is involved in the regulation of feeding and reproductive behaviors (Sandeman et al., 1992); and its localization in the olfactory lobe and clusters 9, 10 and 11 of the deutocerebrum revealed that *Sp*-AST-C is associated with the modulation of the visual and chemosensory process, and involved in the regulation on feeding behaviors (Urlacher et al., 2016; Urlacher et al., 2017).

In crustaceans, information on the functions of C-type AST is still scanty although it was identified almost a decade ago (Dickinson et al., 2009). In this study, the tissue distribution of *Sp-AST-CR* in *S. paramamosain* may provide a cue to understanding the potential roles played by C-type AST in crustaceans. In insect species, it is believed that the C-type ASTs are pleiotropic peptides that are involved in various metabolic roles (Stay and Tobe, 2007). This is further supported by the extensive expression of C-type AST receptor in many tissues/organs. For instance, in *T. castaneum*, *TC-AST-CR* transcript was widely expressed in the head, gut, corpora allata, fat body and the reproductive organs (Audsley et al., 2013). Similarly, in *S. paramamosain*, RT-qPCR showed that *Sp-AST-CR* was broadly present in the detected tissues except the eyestalk ganglion and hepatopancreas (Fig. 3). In Lepidoptera, e.g. *M. sexta* and *A. aegypti*, AST-C can block JH synthesis in the corpora allata (Kramer et al., 1991; Nouzova et al., 2015). In crustaceans, there is a homologous gland to the corpora allata, namely the mandibular organ, which can produce an equivalent hormone to JH, i.e. MF (Miyakawa et al., 2014). In adult female *D. melanogaster*, inhibition of C-type AST receptor-1 or -2 by RNA interference resulted in an increase of MF and JH III biosynthesis (Wang et al., 2012). Currently, there is no evidence to suggest that

Journal of Experimental Biology (2019) 222, jeb207985. doi:10.1242/jeb.207985

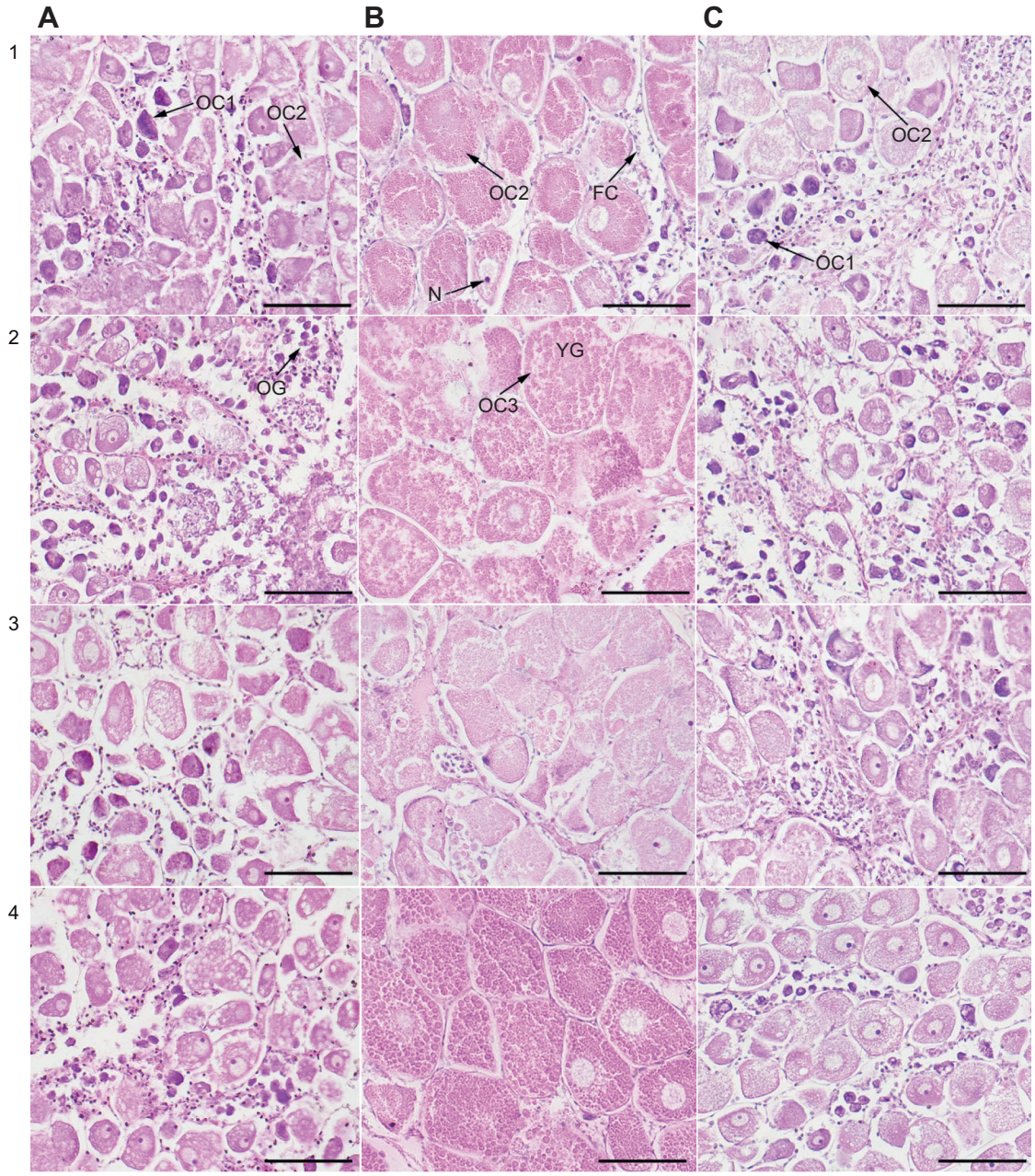

Fig. 8. Histological changes in *S. paramamosain* ovary at the early vitellogenic stage in response to administration of synthetic *Sp*-AST-C peptide. (A) Pre-injection control. (B) Crab saline treatment (saline control). (C) *Sp*-AST-C peptide treatment. Images are from *n*=4 crabs for each condition. OG, oogonium; OC1, previtellogenic oocyte; OC2, early vitellogenic oocyte; OC3, late vitellogenic oocyte; N, cell nucleus; YG, yolk granule. Scale bars: 100 μm.

C-type ASTs act as inhibitors of MF production in crustaceans, but the presence of *Sp-AST-CR* transcript in the mandibular organ of *S. paramamosain* indicates that C-type AST is potentially involved in the regulation of MF production. In *H. americanus*, it was reported that the AST-C receptor was expressed in the heart and C-type AST was able to modulate the output of the heart (Dickinson et al., 2009). In the present study, the existence of *Sp-AST-CR* transcript in the heart implied a similar regulation of C-type AST in the heart of *S. paramamosain*. In addition, in *T. castaneum*, *in vitro* assay revealed that *Tc*-AST-C stimulated the release of proteases from the anterior midgut in a dose-dependent manner (Audsley et al., 2013). In *S. paramamosain*, both *Sp-AST-C* and *Sp-AST-CR* transcripts were detected in the middle gut, which suggests that it might impact on the same activities as in the gut. Surprisingly, *Sp-AST-CR* was highly expressed in the Y-organ of *S. paramamosain*, the site of ecdysone biosynthesis in crustaceans. Up to now, the expression of *Sp-AST-CR* in the Y-organ has never been studied. In *B. mori*, studies have shown that the B-type ASTs are a potent inhibitory factor for ecdysone biosynthesis (Davis et al., 2003; Yamanaka et al., 2010). Collectively, our results indicate that C-type AST is probably involved in the regulation of ecdysone biosynthesis. In our previous study, qPCR results showed that the level of *Sp*-AST-C precursor expression in the cerebral ganglion declined gradually during ovarian development, indicating it might be a negative regulatory factor of vitellogenesis (Bao et al., 2015). Interestingly, in the present study, we found that *Sp-AST-CR* transcript was expressed in the ovary of *S. paramamosain* and its expression pattern during ovarian development was similar to that of *Sp-AST-C* (Fig. 3B), which

Journal of Experimental Biology (2019) 222, jeb207985. doi:10.1242/jeb.207985

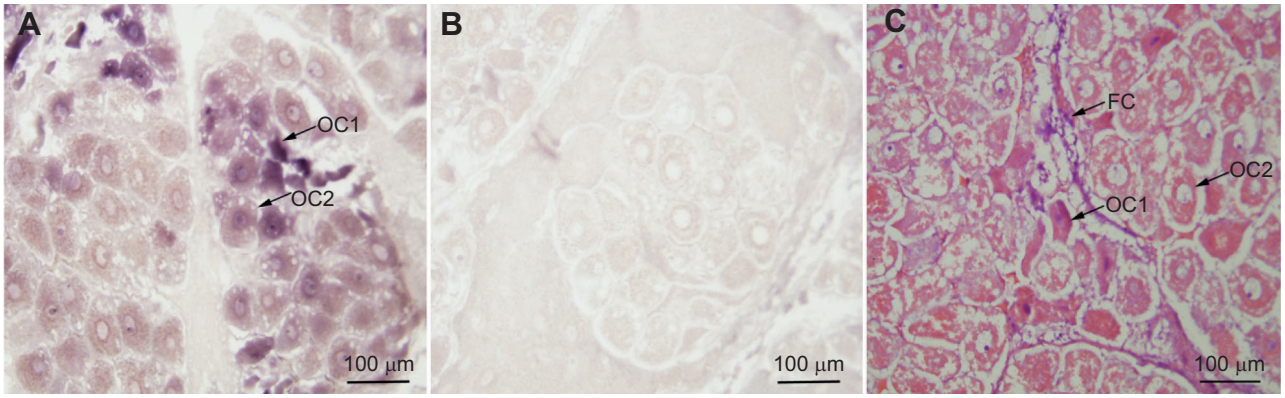

Fig. 9. Localization of *Sp-AST-CR* in *S. paramamosain* ovary at the early vitellogenic stage. (A) Localization of *Sp-AST-CR* mRNA by the antisense probe; arrows indicate the positive signals of *Sp-AST-CR* in the oocytes. (B) Negative control result with the sense probe. (C) Hematoxylin and Eosin staining. OC1, previtellogenic oocyte; OC2, early vitellogenic oocyte; FC, follicular cell.

further revealed that the ovary was under the direct control of C-type ASTs. In summary, the widespread distribution of *Sp-AST-CR* in *S. paramamosain* suggests that C-type AST might have multiple functions in crustaceans as well as in insects.

To further investigate the effect of *Sp*-AST-C on vitellogenesis of *S. paramamosain*, both *in vitro* and *in vivo* experiments were conducted in the present study. Vg, a precursor of vitellus, is synthesized in the hepatopancreas and the ovary, and subsequently taken up by analysis of the the oocytes via endocytosis mediated by the Vg receptor (Warrier and Subramoniam, 2002); this process is termed vitellogenesis. Thus, we used *Sp-Vg* and *Sp-VgR* as indicators of vitellogenesis in this study. The *in vitro* result showed that *Sp*-AST-C peptide significantly reduced the level of *Sp-VgR* transcript in a dose-dependent manner, while it had no effect on the levels of *Sp-Vg* transcript in the ovary and hepatopancreas (Fig. 6). A reduction in the levels of *Sp-VgR* in the ovary was also observed after administration of short neuropeptide F and knockdown of the bone morphogenetic protein 7 receptors by RNA interference (Bao et al., 2018; Shu et al., 2016). Our results suggest that *Sp*-AST-C peptide might inhibit vitellogenesis by impacting on the uptake of Vg by oocytes but not the production of Vg. This was further consolidated by our *in vivo* evidence, which revealed that the expression of *Sp-VgR* and the content of Vn in the ovary were reduced by injection of *Sp*-AST-C (Fig. 7B,C). Furthermore, oocyte diameter and the number of yolk granules in the oocytes decreased after administration of *Sp*-AST-C (Fig. 8), suggesting that oocyte growth was inhibited by *Sp*-AST-C. In *Diploptera punctata*, injection of A-type AST peptide inhibits JH synthesis and oocyte growth (Garside et al., 2000). Thus, in the present study, the inhibition of oocyte growth could alternatively have been caused by the low MF titer in hemolymph. As *Sp*-AST-CR exists in the mandibular organ (Fig. 3A), is possible that injection of *Sp*-AST-C decreased MF titer in the hemolymph; unfortunately, this was not determined, so no conclusion can be made. Nevertheless, our results clearly demonstrate that *Sp-AST-C* had an inhibitory role in Vg absorption and oocyte growth. Finally, given the absence of *Sp-AST-C* mRNA in the ovary and the localization of *Sp-AST-CR* mRNA in the oocytes (Fig. 9), we believe that *Sp*-AST-C acts as a circulating hormone to inhibit the uptake of Vg by oocytes directly.

In conclusion, the extensive distribution of both C-type AST and its putative receptor in the mud crab *S. paramamosain* indicates that *Sp*-AST-C might be a pleiotropic peptide involved in many physiological functions. The *in vitro* and *in vivo* experiment further provide the first evidence that *Sp*-AST-C serves as a circulating hormone to regulate ovarian development via direct inhibition of Vg absorption by oocytes and obstruction of oocyte growth.

Acknowledgements
The authors would like to thank the anonymous reviewers for their helpful suggestions on the manuscript.

Competing interests
The authors declare no competing or financial interests.

Author contributions
Methodology: A.L., H.Y.; Formal analysis: A.L., F.L., W.S.; Investigation: A.L., F.L., W.S.; Data curation: A.L., F.L.; Writing - original draft: A.L., H.Y.; Writing - review & editing: H.H., G.W., H.Y.; Funding acquisition: H.H., G.W., H.Y.

Funding
This study was supported by the National Natural Science Foundation of China (grant numbers: 31972765 and 31772827) and the Fujian Provincial Project of Science and Technology (grant number: 2017N0030).

Data availability
Sp-Vg (FJ812090.1), *Sp-VgR* (KF860893.1), *Sp-AST-C* (MK314113) and *Sp-AST-CR* (MK314114) sequences have been deposited in GenBank.

References
Abdel-Latief, M. and Hoffmann, K. H. (2010). Neuropeptide regulators of the juvenile hormone biosynthesis (*in vitro*) in the beetle, *Tenebrio molitor* (Coleoptera, Tenebrionidae). *Arch. Insect Biochem. Physiol.* **74**, 135-146. doi:10.1002/arch.20359

Audsley, N., Vandersmissen, H. P., Weaver, R., Dani, P., Matthews, J., Down, R., Vuerinckx, K., Kim, Y.-J. and Vanden Broeck, J. (2013). Characterisation and tissue distribution of the PISCF allatostatin receptor in the red flour beetle, *Tribolium castaneum*. *Insect Biochem. Mol. Biol.* **43**, 65-74. doi:10.1016/j.ibmb.2012.09.007

Bachtel, N. D., Hovsepian, G. A., Nixon, D. F. and Eleftherianos, I. (2018). Allatostatin C modulates nociception and immunity in *Drosophila*. *Sci. Rep.* **8**, 7501. doi:10.1038/s41598-018-25855-1

Bao, C., Yang, Y., Huang, H. and Ye, H. (2015). Neuropeptides in the cerebral ganglia of the mud crab, *Scylla paramamosain*: transcriptomic analysis and expression profiles during vitellogenesis. *Sci. Rep.* **5**, 17055. doi:10.1038/srep17055

Bao, C., Yang, Y., Huang, H. and Ye, H. (2018). Inhibitory role of the mud crab short neuropeptide F in vitellogenesis and oocyte maturation via autocrine/paracrine signaling. *Front. Endocrinol.* **9**, 390. doi:10.3389/fendo.2018.00390

Christie, A. E., Stemmler, E. A., Peguero, B., Messinger, D. I., Provencher, H. L., Scheerlinck, P., Hsu, Y.-W. A., Maureen, E., Guiney, M. E., de la Iglesia, H. O. et al. (2006). Identification, physiological actions, and distribution of VYRKPPFNGSIFamide (Val1-SIFamide) in the stomatogastric nervous system of the American lobster *Homarus americanus*. *J. Comp. Neurol.* **496**, 406-421. doi:10.1002/cne.20932

Davis, N. T., Blackburn, M. B., Golubeva, E. G. and Hildebrand, J. G. (2003). Localization of myoinhibitory peptide immunoreactivity in *Manduca sexta* and

B*ombyx mori*, with indications that the peptide has a role in molting and ecdysis. *J. Exp. Biol.* **206**, 1449-1460. doi:10.1242/jeb.00234

Diaz, M. M., Schlichting, M., Abruzzi, K. C., Long, X. and Rosbash, M. (2019). Allatostatin-C/AstC-R2 is a novel pathway to modulate the circadian activity pattern in *Drosophila*. *Curr. Biol.* **29**, 13-22.e3. doi:10.1016/j.cub.2018.11.005

Dickinson, P. S., Wiwatpanit, T., Gabranski, E. R., Ackerman, R. J., Stevens, J. S., Cashman, C. R., Stemmler, E. A. and Christie, A. E. (2009). Identification of SYWKQCAFNAVSCFamide: a broadly conserved crustacean C-type allatostatin-like peptide with both neuromodulatory and cardioactive properties. *J. Exp. Biol.* **212**, 1140-1152. doi:10.1242/jeb.028621

Garside, C. S., Nachman, R. J. and Tobe, S. S. (2000). Injection of Dip-allatostatin or Dip-allatostatin pseudopeptides into mated female Diploptera punctata inhibits endogenous rates of JH biosynthesis and basal oocyte growth. *Insect Biochem. Mol. Biol.* **30**, 703-710. doi:10.1016/S0965-1748(00)00041-2

Hama, H., Kurokawa, H., Kawano, H., Ando, R., Shimogori, T., Noda, H., Fukami, K., Sakaue-Sawano, A. and Miyawaki, A. (2011). Scale: a chemical approach for fluorescence imaging and reconstruction of transparent mouse brain. *Nat. Neurosci.* **14**, 1481. doi:10.1038/nn.2928

Huang, X., Ye, H., Huang, H., Yang, Y. and Gong, J. (2014). An insulin-like androgenic gland hormone gene in the mud crab, *Scylla paramamosain*, extensively expressed and involved in the processes of growth and female reproduction. *Gen. Comp. Endocrinol.* **204**, 229-238. doi:10.1016/j.ygcen.2014.06.002

Huang, X., Feng, B., Huang, H. and Ye, H. (2017). In vitro stimulation of vitellogenin expression by insulin in the mud crab, Scylla paramamosain, mediated through PI3K/Akt/TOR pathway. *Gen. Comp. Endocr.* **250**, 175-180. doi:10.1016/j.ygcen.2017.06.013

Kramer, S. J., Toschi, A., Miller, C. A., Kataoka, H., Quistad, G. B., Li, J. P., Carney, R. L. and Schooley, D. A. (1991). Identification of an allatostatin from the tobacco hornworm *Manduca sexta*. *Proc. Natl. Acad. Sci. USA* **88**, 9458-9462. doi:10.1073/pnas.88.21.9458

Kreienkamp, H.-J., Larusson, H. J., Witte, I., Roeder, T., Birgül, N., Hönck, H.-H., Harder, S., Ellinghausen, G., Buck, F. and Richter, D. (2002). Functional annotation of two orphan G-protein-coupled receptors, Drostar1 and -2, from *Drosophila melanogaster* and their ligands by reverse pharmacology. *J. Biol. Chem.* **277**, 39937-39943. doi:10.1074/jbc.M206931200

Li, Y. P., Hernandez-Martinez, S. and Noriega, F. G. (2004). Inhibition of juvenile hormone biosynthesis in mosquitoes: effect of allatostatic head factors, PISCF- and YXFGL-amide-allatostatins. *Regul. Peptides* **118**, 175-182. doi:10.1016/j.regpep.2003.12.004

Li, Y. P., Hernandez-Martinez, S., Fernandez, F., Mayoral, J. G., Topalis, P., Priestap, H., Perez, M., Arti Navare, A. and Noriega, F. G. (2006). Biochemical, molecular, and functional characterization of PISCF-allatostatin, a regulator of juvenile hormone biosynthesis in the mosquito *Aedes aegypti*. *J. Biol. Chem.* **281**, 34048-34055. doi:10.1074/jbc.M606341200

Liu, A., Liu, J., Liu, F., Huang, Y. Y., Wang, G. Z. and Ye, H. H. (2018). Crustacean female sex hormone from the mud crab *Scylla paramamosain* is highly expressed in prepubertal males and inhibits the development of androgenic gland. *Front. Physiol.* **9**, 924. doi:10.3389/fphys.2018.00924

Lorenz, M. W., Kellner, R. and Hoffmann, K. H. (1995). A family of neuropeptides that inhibit juvenile hormone biosynthesis in the cricket, *Gryllus bimaculatus*. *J. Biol. Chem.* **270**, 21103-21108. doi:10.1074/jbc.270.36.21103

Lorenz, M. W., Kellner, R. and Hoffmann, K. H. (1999). Allatostatins in *Gryllus bimaculatus* (Ensifera: Gryllidae): new structures and physiological properties. *Eur. J. Entomol.* **96**, 267-274. doi:10.1111/j.1365-3032.2001.00217.x

Ma, M., Szabo, T. M., Jia, C., Marder, E. and Li, L. (2009). Mass spectrometric characterization and physiological actions of novel crustacean C-type allatostatins. *Peptides* **30**, 1660-1668. doi:10.1016/j.peptides.2009.05.023

Matthews, H. J., Audsley, N. and Weaver, R. J. (2007). Interactions between allatostatins and allatotropin on spontaneous contractions of the foregut of larval *Lacanobia oleracea*. *J. Insect Physiol.* **53**, 75-83. doi:10.1016/j.jinsphys.2006.10.007

Mayoral, J. G., Nouzova, M., Brockhoff, A., Goodwin, M., Hernandez-Martinez, S., Richter, D., Meyerhof, W. and Noriega, F. G. (2010). Allatostatin-C receptors in mosquitoes. *Peptides* **31**, 442-450. doi:10.1016/j.peptides.2009.04.013

Miyakawa, H., Toyota, K., Sumiya, E. and Iguchi, T. (2014). Comparison of JH signaling in insects and crustaceans. *Curr. Opin. Insect Sci.* **1**, 81-87. doi:10.1016/j.cois.2014.04.006

Nagaraju, G. P. C. (2011). Reproductive regulators in decapod crustaceans: an overview. *J. Exp. Biol.* **214**, 3-16. doi:10.1242/jeb.047183

Nouzova, M., Rivera-Perez, C. and Noriega, F. G. (2015). Allatostatin-C reversibly blocks the transport of citrate out of the mitochondria and inhibits juvenile hormone synthesis in mosquitoes. *Insect Biochem. Mol. Biol.* **57**, 20-26. doi:10.1016/j.ibmb.2014.12.003

Oeh, U., Lorenz, M. W., Dyker, H., Lösel, P. and Hoffmann, K. H. (2000). Interaction between Manduca sexta allatotropin and Manduca sexta allatostatin in the fall armyworm *Spodoptera frugiperda*. *Insect Biochem. Mol. Biol.* **30**, 719-727. doi:10.1016/S0965-1748(00)00043-6

Olias, G., Viollet, C., Kusserow, H., Epelbaum, J. and Meyerhof, W. (2004). Regulation and function of somatostatin receptors. *J. Neurochem.* **89**, 1057-1091. doi:10.1111/j.1471-4159.2004.02402.x

Pratt, G. E., Farnsworth, D. E., Siegel, N. R., Fok, K. F. and Feyereisen, R. (1989). Identification of an allatostatin from adult *Diploptera punctata*. *Biochem. Biophys. Res. Commun.* **163**, 1243-1247. doi:10.1016/0006-291X(89)91111-X

Saetan, J., Kruangkum, T., Phanthong, P., Tipbunjong, C., Udomuksorn, W., Sobhon, P. and Sretarugsa, P. (2018). Molecular cloning and distribution of oxytocin/vasopressin-like mRNA in the blue swimming crab, *Portunus pelagicus*, and its inhibitory effect on ovarian steroid release. *Comp. Biochem. Physiol. A Mol. Integr. Physiol.* **218**, 46-55. doi:10.1016/j.cbpa.2018.01.012

Sandeman, D., Sandeman, R., Derby, C. and Schmidt, M. (1992). Morphology of the brain of crayfish, crabs, and spiny lobsters: a common nomenclature for homologous structures. *Biol. Bull.* **183**, 304-326. doi:10.2307/1542217

Shu, L., Yang, Y. N., Huang, H. Y. and Ye, H. H. (2016). A bone morphogenetic protein ligand and receptors in mud crab: A potential role in the ovarian development. *Mol. Cell. Endocrinol.* **434**, 99-107. doi:10.1016/j.mce.2016.06.023

Stanhope, M., Lameyer, T. J., Shea, D. N., Chi, M., Pascual, M. G., Schulz, D. J., Christie, A. E. and Dickinson, P. S. (2016). Mechanisms underlying differential responses to the neuropeptide Allatostatin-C (AST-C) in the cardiac ganglion of the lobster, *Homarus americanus*. *FASEB J.* **30**, 760-761. doi:10.1371/journal.pone.0145964

Stay, B. and Tobe, S. S. (2007). The role of allatostatins in juvenile hormone synthesis in insects and crustaceans. *Annu. Rev. Entomol.* **52**, 277-299. doi:10.1146/annurev.ento.51.110104.151050

Stemmler, E. A., Bruns, E. A., Cashman, C. R., Dickinson, P. S. and Christie, A. E. (2010). Molecular and mass spectral identification of the broadly conserved decapod crustacean neuropeptide pQIRYHQCYFNPISCF: the first PISCF-allatostatin (Manduca sexta- or C-type allatostatin) from a non-insect. *Gen. Comp. Endocrinol.* **165**, 1-10. doi:10.1016/j.ygcen.2009.05.010

Urlacher, E., Soustelle, L., Parmentier, M.-L., Verlinden, H., Gherardi, M.-J., Fourmy, D., Mercer, A. R., Devaud, J.-M. and Massou, I. (2016). Honey bee allatostatins target galanin/somatostatin-like receptors and modulate learning: a conserved function? *PLoS ONE* **11**, e0146248. doi:10.1371/journal.pone.0146248

Urlacher, E., Devaud, J.-M. and Mercer, A. R. (2017). C-type allatostatins mimic stress-related effects of alarm pheromone on honey bee learning and memory recall. *PLoS ONE* **12**, e0174321. doi:10.1371/journal.pone.0174321

Veenstra, J. A. (2009). Allatostatin C and its paralog allatostatin double C: the arthropod somatostatins. *Insect Biochem. Mol. Biol.* **39**, 161-170. doi:10.1016/j.ibmb.2008.10.014

Veenstra, J. A. (2016). Allatostatins C, double C and triple C, the result of a local gene triplication in an ancestral arthropod. *Gen. Comp. Endocrinol.* **230-231**, 153-157. doi:10.1016/j.ygcen.2016.04.013

Verlinden, H., Gijbels, M., Lismont, E., Lenaerts, C., Broeck, J. V. and Marchal, E. (2015). The pleiotropic allatoregulatory neuropeptides and their receptors: a mini-review. *J. Insect Physiol.* **80**, 2-14. doi:10.1016/j.jinsphys.2015.04.004

Walsh, P., Pong, S., Armstrong, M., Christie, A. E. and Dickinson, P. S. (2017). Characterization of the receptors associated with the differing responses to the neuropeptide, AST-C, by the cardiac ganglion of the American Lobster, *Homarus americanus*. *FASEB J.* **31**, 874-876.

Wang, C., Zhang, J., Tobe, S. S. and Bendena, W. G. (2012). Defining the contribution of select neuropeptides and their receptors in regulating sesquiterpenoid biosynthesis by *Drosophila melanogaster* ring gland/corpus allatum through RNAi analysis. *Gen. Comp. Endocrinol.* **176**, 347-353. doi:10.1016/j.ygcen.2011.12.039

Warrier, S. and Subramoniam, T. (2002). Receptor mediated yolk protein uptake in the crab *Scylla serrata*: crustacean vitellogenin receptor recognizes related mammalian serum lipoproteins. *Mol. Reprod. Dev.* **61**, 536-548. doi:10.1002/mrd.10106

Williamson, M., Lenz, C., Winther, M. E., Nässel, D. R. and. Grimmelikhuijzen, C. J. P. (2001). Molecular cloning, genomic organization, and expression of a C-type (Manduca sexta-type) allatostatin preprohormone from *Drosophila melanogaster*. *Biochem. Biophys. Res. Commun.* **282**, 124-130. doi:10.1006/bbrc.2001.4565

Wilson, C. H. and Christie, A. E. (2010). Distribution of C-type allatostatin (C-AST)-like immunoreactivity in the central nervous system of the copepod *Calanus finmarchicus*. *Gen. Comp. Endocrinol.* **167**, 252-260. doi:10.1016/j.ygcen.2010.03.012

Wiwatpanit, T., Powers, B. and Dickinson, P. S. (2012). Inter-animal variability in the effects of C-type allatostatin on the cardiac neuromuscular system in the lobster *Homarus americanus*. *J. Exp. Biol.* **215**, 2308-2318. doi:10.1242/jeb.069989

Yamanaka, N., Yamamoto, S., Žitňan, D., Watanabe, K., Kawada, T., Satake, H., Kaneko, Y., Hiruma, K., Yoshiaki, T., Shinoda, T. et al. (2008). Neuropeptide receptor transcriptome reveals unidentified neuroendocrine pathways. *PLoS ONE* **3**, e3048. doi:10.1371/journal.pone.0003048

Yamanaka, N., Hua, Y. J., Roller, L., Spalovská-Valachová, I., Mizoguchi, A., Kataoka, H. and Tanaka, Y. (2010). *Bombyx* prothoracicostatic peptides activate the sex peptide receptor to regulate ecdysteroid biosynthesis. *Proc. Natl. Acad. Sci.USA* **107**, 2060-2065. doi:10.1073/pnas.0907471107

Zhang, Y., Wu, X., Yang, F., Liu, Z. and Cheng, Y. (2011). Purification of vitellin and ELISA determination of vitellin of swimming crab (*Portunus trituberculatus*). *J. Fish. Chin.* **35**, 1146-1157.

Zmora, N., Trant, J., Chan, S. M. and Chung, J. S. (2007). Vitellogenin and its messenger RNA during ovarian development in the female blue crab, Callinectes sapidus: gene expression, synthesis, transport, and cleavage. *Biol. Reprod.* **77**, 138-146. doi:10.1095/biolreprod.106.055483